High Resolution Imaging Mass Spectrometry of Human Donor Eyes with Retinal Pathology

David M.G. Anderson[1], Ankita Kotnala[1,2], Jarod Fincher[1], Jeffrey D. Messinger[2], Nathan Heath Patterson[1], Jeffrey M. Spraggins[1], Christine A. Curcio[2], Richard M. Caprioli[1], and Kevin L. Schey[1].

1. Department of Biochemistry, Vanderbilt University, Nashville, TN. **2.** Department of Ophthalmology, University of Alabama at Birmingham, Birmingham, AL.

Overview: We sought high spatial and mass resolution imaging mass spectrometry (IMS) methods for imaging molecular changes in chorioretinal tissue from donors with retinal pathology to elucidate molecules present in drusen, basal laminar deposits and migrating RPE cells.

Introduction: Age-related macular degeneration (AMD) is a leading cause of legal blindness in the elderly and is increasing as the population ages. Death of photoreceptors and vision loss has been linked to extracellular deposits on apical and basal aspects of the retinal pigment epithelium (RPE); a single cell layer that supports the photoreceptors. The purpose of this study is to use high spatial and mass resolution imaging mass spectrometry (IMS) to molecularly characterize regions of pathology observed in drusen, basal laminar deposits, RPE cells migrating out of their layer, and neurosensory retina.

Methods: 12-14 µm sections of fixed and frozen human donor tissue were prepared as shown in panel 1 A. Sections were mounted on poly-lysine coated ITO slides. Autofluorescence images of dried tissue sections were taken prior to matrix application. The matrix 1,5-diaminonaphalene (DAN) was applied using an in-house sublimation device prior to negative ion mode analysis. MALDI IMS data were acquired with a 10-15 µm pixel size in full scan mode using a solariX 9.4T FT ICR mass spectrometer (Bruker Daltonics) equipped with a modified source to provide higher spatial resolution. Migrating RPE data were acquired with a Prototype MALDI timsTOF Flex[1] (Bruker Daltonics). Cholesterol analysis was performed with tissue sections sprayed with 200mM Na_3PO_4 using a HTX TM sprayer with 3 passes at 0.05 mL/min to promote the formation of sodium adducts of neutral species such as cholesterol and cholesterol esters. The MALDI matrix DHB was also applied to aid in the desorption of sodium adducts and analytes using a in-house sublimation apparatus heated 130°C for 3.5 minutes. Finally 10 nm of gold wass added using a sputter coater (Ted Pella, Cressington) to aid in desorption and prevent charge accumulation [2,3]. Data acquisition was performed in positive ion mode with a 15 µm pixel size using a Bruker solariX 9.4T FT ICR mass spectrometer.

Following data acquisition, a highly accurate image registration workflow (Panel 1, 6) [4] was performed using several imaging modalities. Data were reconstructed using ImageJ Fiji freeware (NIH) for images in panels 2 and 4. Images which are not overlaid in panel 2 and 3 were generated using flexImaging (Bruker Daltonics). MALDI IMS images in panel 5 were generated using SCiLS software. Identifications were based on accurate mass using LC-MS/MS data with manual interpretation of MS/MS spectra.

Panel 1. Sample Procurement and Preparation.

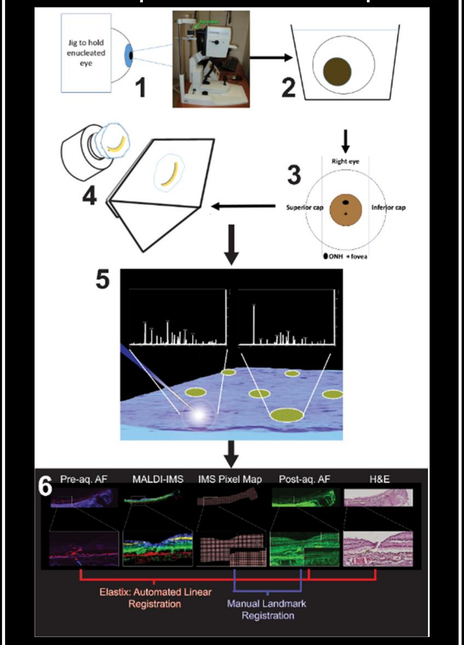

Figure 1. Workflow of sample preparation and multimodal imaging. 1. Whole eye mounted in jig to obtain OCT image. **2.** The cornea is removed before fixation with 4% paraformaldehyde for 48 hours at 4°C. **3.** The eye is placed in a dissection guide as described in the text to capture a belt of tissue containing the optic nerve, macula, and temporal periphery. The belt is embedded in 2.6% CMC in a cryomold. The caps are discarded. **4.** Cryosections at 12-14 µm throughout the belt are thaw-mounted on either glass or ITO slides. **5.** ITO slides are imaged for autofluorescence (AF) before being coated with matrix via sublimation for acquisition of IMS data. **6.** Highly accurate data registration is performed from IMS, post-acquisition AF, pre AF, and H&E stained tissue.

Panel 2. Drusen Lipids in Fresh Tissue

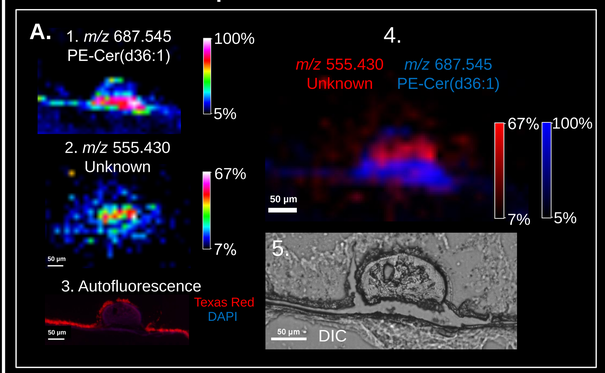

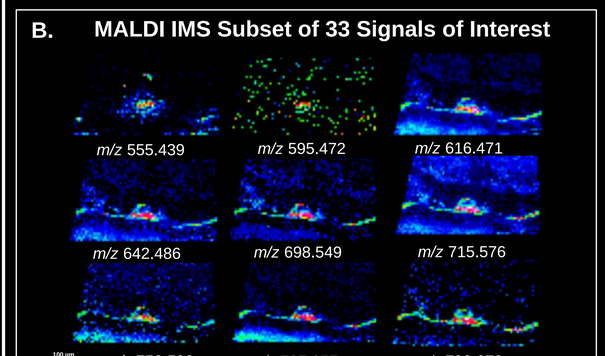

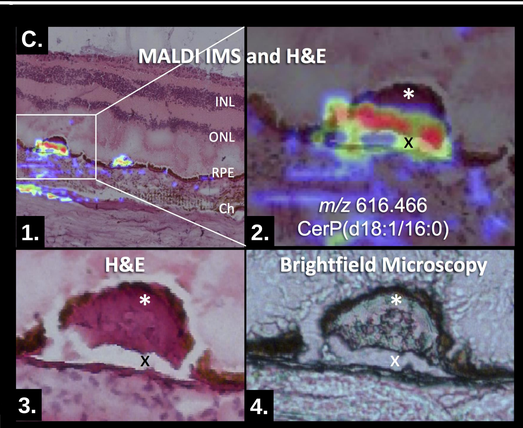

Panel 2 demonstrates novelty and heterogeneity in drusen lipids via IMS, including a newly observed phosphatidyl ethanolamine ceramide phosphate (red, **Panel 2A1**) once overlaid with an unidentified signal at *m/z* variation in the localization clearly indicates heterogenicity observed within this particular druse. These data demonstrate our ability to detect multiple lipid species from deposits (Panel 2B) and identify specific lipids in deposits of interest (drusen) using this workflow. By combining imaging modalities identifying and localizing signals to both retinal layers and AMD pathology is demonstrated in Panel 2C. As it is important to independently verify druse integrity a multi modal imaging approach is necessary, as biomechanically fragile soft drusen can be lost in processing [10]. **Panel 2A3-5 and C1-4**) show autofluorescence, DIC, and bright-field microscopy confirming pathology is present.

Panel 3. Salt Solution DHB Analysis of Druse for Cholesterol and Unesterified Cholesterol

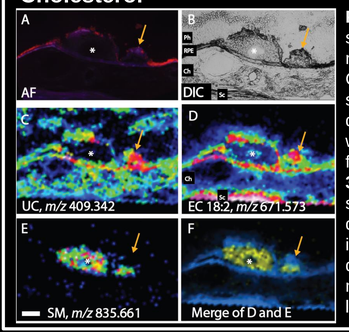

Panel 3 shows drusen from a 90-year-old female donor. **Panel 3A** shows AF (red) of two RPE elevations (* and →) with druse contents revealed by differential interference contrast microscopy (**Fig. 5B;** Ph, Ch, Sc, photoreceptors, choroid, sclera, respectively). **Panel 3C** shows cholesterol ([M+Na]+ ion, m/z 409) in BrM and the smaller druse, with additional signal in photoreceptors and choroid consistent with cellular membranes [12]. In contrast, cholesterol esterified to the fatty acid linoleate (18:2, [M+Na]+ ion , m/z 671.573) shown in **Panel 3D** appears in the druse, BrM, and sclera. **Panel 3E-F** show a sphingomyelin adducted to a sodium ion (SM(d18:2_24:1)Na^+) in the druse interior only, making it the most specifically localized druse lipid identified to date. The absence of this signal in BrM suggests that the druse internal environment or the environment of druse-impacted RPE might promote transformation of compounds in the sub-RPE-basal lamina space [13].

Panel 4. MALDI IMS 93 Year Old AMD Eye With Basal Laminar Deposit

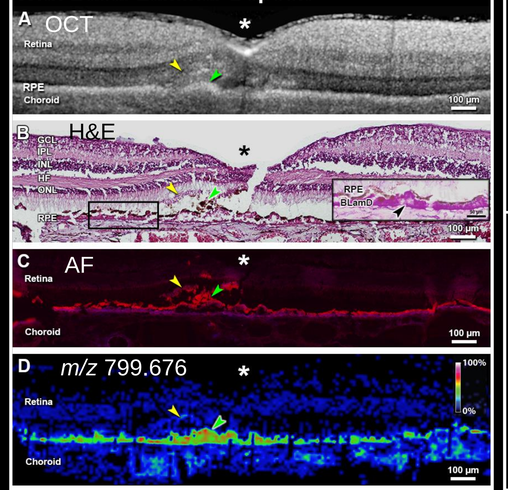

Panel. 2A *ex vivo* OCT of an eye from a 93-yr-old female donor with AMD shows hyperreflective foci (yellow arrowhead) and an RPE elevation (green arrowhead) near the fovea (*). **Panel 2B** shows that retinal layers are visible in sections stained with H&E after IMS interrogation; inset magnifies BLamD (periodic acid Schiff-hematoxylin staining of an alternate section). **Panel 2C** shows autofluorescence (AF) of the elevated RPE layer and anteriorly migrated RPE. **Panel 2D** shows a PE-Cer NMe2(42:1) lipid of m/z=799.671 [5] localizing to BLamD, building on previous histochemistry findings of lipids in this deposit [6]. The ability to detect BLamD and to determine its molecular composition is important and timely, because the effects of BLamD, an early-identified histologic risk factor for AMD progression [7], are just now being recognized clinically [7-8]. Also, several mouse models of inherited retinopathies have BLamD [9].

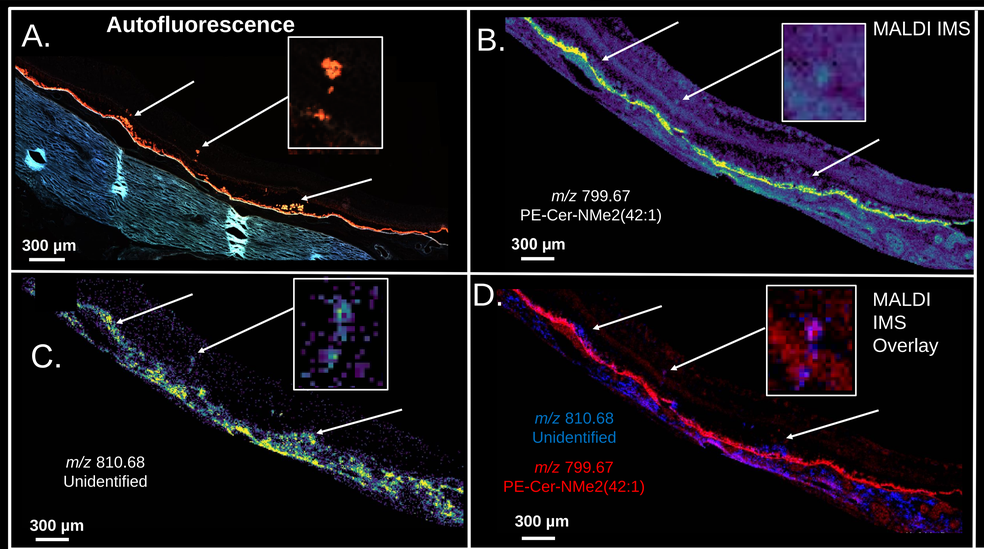

Panel 5. Migrating RPE

Panel 5 A displays autofluorescence from an 80 year old donor eye section which displays autofluorescent lipofuscin within RPE cells that migrated into the neurosensory retina (areas indicated with arrows). Panel 5B displays the same PE-Cer-NMe2(42:1) observed in the basal laminar deposit in panel 4 with high signal observed in the RPE layer of the tissue and lower intensity in migrating RPE cell (zoomed inset). Panel 5C displays an unidentified signal at m/z 810.68 that localizes to the choroid, regions displaying high autofluorescence, and migrating RPE cells indicated by the zoomed inset. Once these signals are overlaid in panel 5D, the relative abundances and localizations in these areas of interest can be more clearly observed.

Conclusions: MALDI IMS combined with multimodal imaging from autofluorescence, brightfield microscopy, and OCT imaging provides a powerful tool to elucidate the molecular composition observed in discrete layers of specific AMD pathology as well as in the neural retina.

Acknowledgements: This project was supported by the National Institutes of Health P41 GM103391 (RMC) and R01 EY027948 (CC).

1. Spraggins, J. M.; Djambazova, K. V.; Rivera, E. S.; Migas, L. G.; Neumann, E. K.; Fuetterer, A.; Suetering, J.; Goedecke, N.; Ly, A.; Van de Plas, R.; Caprioli, R. M., High-Performance Molecular Imaging with MALDI Trapped Ion-Mobility Time-of-Flight (timsTOF) Mass Spectrometry. *Analytical Chemistry 2019, 91* (22), 14552-14560.
2. Dufresne, M.; Masson, J.-F.; Chaurand, P., Sodium-Doped Gold-Assisted Laser Desorption Ionization for Enhanced Imaging Mass Spectrometry of Triacylglycerols from Thin Tissue Sections. *Analytical Chemistry 2016, 88* (11), 6018-6025.
3. Dufresne, M., Patterson, N. H.; Norris, J. L.; Caprioli, R. M., Combining Salt Doping and Matrix Sublimation for High Spatial Resolution MALDI Imaging Mass Spectrometry of Neutral Lipids. *Analytical Chemistry 2019, 91* (20), 12928-12934.
4. Patterson, N. H.; Tuck, M.; Van de Plas, R.; Caprioli, R. M., Advanced Registration and Analysis of MALDI Imaging Mass Spectrometry Measurements through Autofluorescence Microscopy. *Analytical Chemistry 2018, 90* (21), 12395-12403.
5.Liu A, Chang J, Lin Y, Shen Z, Bernstein PS. Long-chain and very long-chain polyunsaturated fatty acids in ocular aging and age-related macular degeneration. *J Lipid Res*. 2011;51:3217–3229.
6.Curcio CA, Presley JB, Malek G, Medeiros NE, Avery DV, Kruth HS. Esterified and unesterified cholesterol in drusen and basal deposits of eyes with age-related maculopathy. *Exp Eye Res*. 2005;81(6):731-741.
7. Sarks SH. Ageing and degeneration in the macular region: a clinico-pathological study. *Br. J. Ophthalmol.* 1976;60(5):324-341.
8. Tan ACS, Astroz P, Dansingani KK, Slakter JS, Yannuzzi LA, Curcio CA, Freund KB. The plateau, an optical coherence tomographic signature of geographic atrophy: evolution, multimodal imaging, and candidate histology. *Invest Ophthalmol Vis Sci*. 2017;58(4):2349–2358.
9. Fu L, Garland D, Yang Z, Shukla D, Rajendran A, Pearson E, Stone EM, Zhang K, Pierce EA. The R345W mutation in EFEMP1 is pathogenic and causes AMD-like deposits in mice. *Human molecular genetics*. 2007;16(20):2411-2422.
10.Rudolf M, Clark ME, Chimenti S, Curcio CA. Prevalence and morphology of druse types in the macula and periphery of eyes with age-related maculopathy. *Invest Ophthalmol Vis Sci*. 2008;49(3):1200-1209.
11. Haimovici R, Gantz DL, Rumelt S, Freddo TF, Small DM. The lipid composition of drusen, Bruch's membrane, and sclera by hot stage polarizing microscopy. *Invest Ophthalmol Vis Sci*. 2001;42(7):1592-1599.
12. Curcio CA, Johnson M, Huang J-D, Rudolf M. Apolipoprotein B-containing lipoproteins in retinal aging and age-related maculopathy. *J. Lipid Res*. 2010;51(3):451-467.
13. Tan AC, Pilgrim M, Fearn S, Bertazzo S, Tsolaki E, Morrell A, Li M, Messinger JD, Dolz-Marco R, Nittala MG, Lei J, Sadda SR, Lengyel I, Freund KB, Curcio CA. Calcified nodules in retinal drusen are associated with disease progression with age-related macular degeneration. *Sci Transl Med*. 2018;10:466-477.

david.m.anderson@vanderbilt.edu